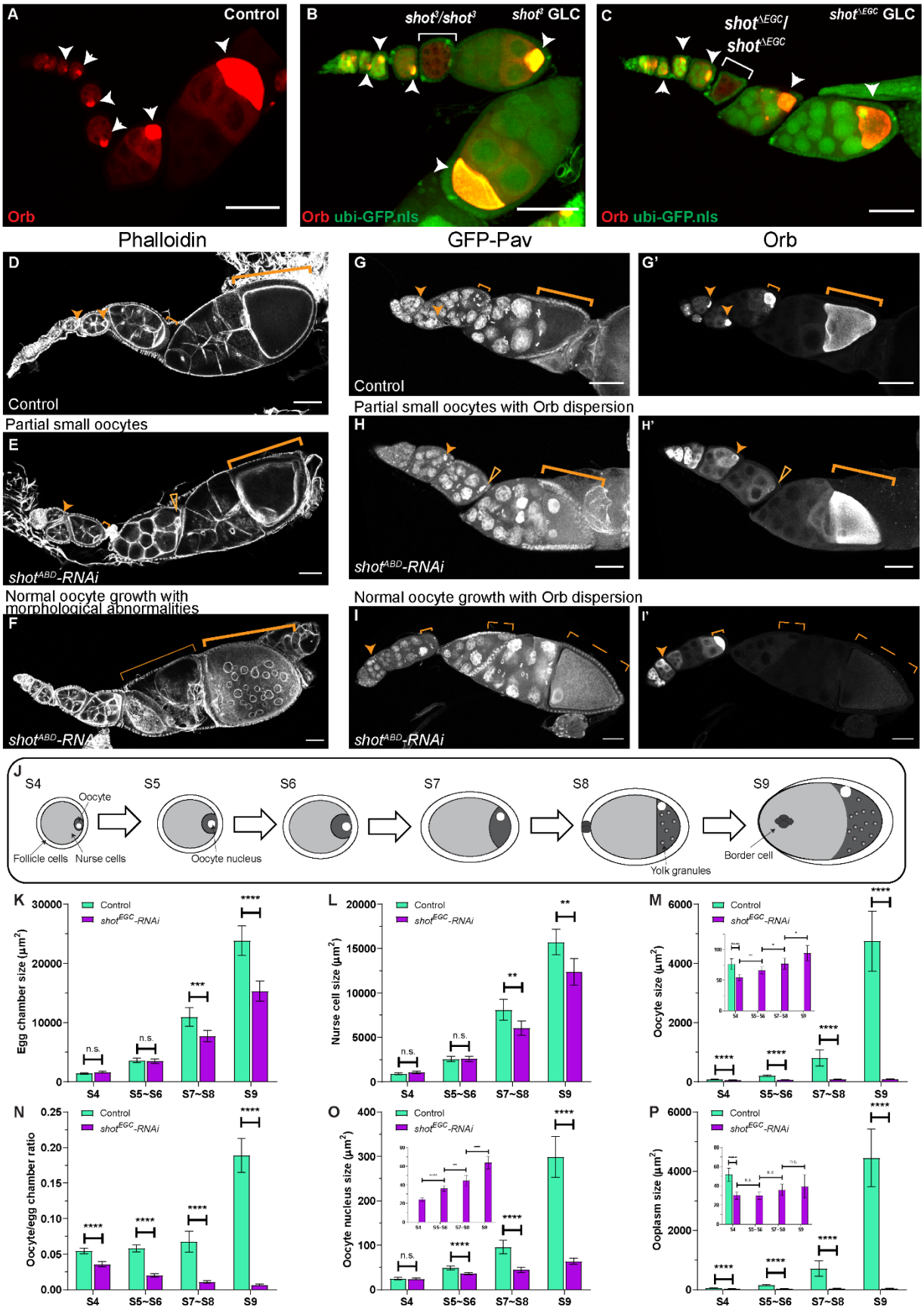
A
Control
Orb
B
shot3/shot3
shot3 GLC
Orb ubi-GFP.nls
C
shotΔEGC/
shotΔEGC
shotΔEGC GLC
Orb ubi-GFP.nls
Phalloidin
GFP-Pav
Orb
D
Control
Partial small oocytes
E
shotABD-RNAi
Normal oocyte growth with
morphological abnormalities
F
shotABD-RNAi
G
Control
G'
Partial small oocytes with Orb dispersion
H
shotABD-RNAi
H'
Normal oocyte growth with Orb dispersion
I
shotABD-RNAi
I'
J
S4
Oocyte
S5
S6
S7
S8
S9
Follicle cells
Nurse cells
Oocyte nucleus
Yolk granules
Border cell
K
Egg chamber size (μm2)
Control
shotEGC-RNAi
n.s.
***
****
S4
S5~S6
S7~S8
S9
L
Nurse cell size (μm2)
n.s.
**
M
Oocyte size (μm2)
****
N
Oocyte/egg chamber ratio
O
Oocyte nucleus size (μm2)
P
Ooplasm size (μm2)

Figure S1. Shot is required for oocyte specification and growth. Related to Figure 1.

(A) Concentrated Orb staining in control oocytes from stage 1 to stage 9. (B) A germline clone that is homozygous of *shot*^{3}, the strongest loss-of-function allele of *shot*, fails to specify the oocyte in the egg chamber, shown by the lack of concentrated Orb staining (white bracket) (100%, N=39). All *shot*^{3} heterozygous egg chambers have normal oocyte specification (white arrowheads) (100%, N=170). (C) A germline clone that is homozygous of *shot*$^{\Delta EGC}$ fails to specify the oocyte in the egg chamber, shown by the lack of concentrated Orb staining (white bracket) (100%, N=98). All *shot*$^{\Delta EGC}$ heterozygous egg chambers have normal oocyte specification (white arrowheads) (100%, N=445).

(D-F) In addition to complete small oocyte phenotype (shown in Figure 1 and Video S1), *shot-RNAi* also display partial small oocytes (E, pointed by the open arrowhead), and normal oocyte growth with morphological abnormalities (F, abnormal nurse cell fusion highlighted by the thin bracket and oocyte actin blebbing highlighted by the thick bracket), compared to normal oogenesis in control (D). Percentages of these phenotypes are summarized in Figure 1F.

(G-I') *shot-RNAi* also display partial small oocytes with Orb dispersion (H-H', pointed by the open arrowhead), and normal oocyte growth with Orb dispersion (I-I', highlighted by the dashed brackets), compared to normal oocyte growth with Orb concentration in control (G-G'). Percentages of these phenotypes are summarized in Figure 1G.

A-I', scale bars, 50 μm.

(J) A cartoon illustration of *Drosophila* egg chamber staging: (1) stage 4: the egg chamber has a spherical shape with blob-like DAPI staining in the nurse cell nucleus; (2) stage 5: the egg chamber slightly elongates along the A-P axis and posterior nurse cells have more DNA staining than anterior nurse cells; (3) stage 6: the egg chamber gets further elongated and oocyte volume increases; less difference in nurse cell DNA contents; (4) stage 7: the nurse cell-oocyte boundary is less curved than stage 6; oocyte polarization starts, with the oocyte nucleus migrating towards the nurse cell-oocyte boundary; (5) stage 8: the nurse cell-oocyte boundary is more flattened; yolk granules become visible in the ooplasm; (6) stage 9: border cells start migration towards the nurse cell-oocyte boundary; follicle cells start to migrate towards the posterior half of the egg chamber.

(K-P) Measurements of egg chambers from stage 4 to stage 9 in control and in *shot*^{EGC}-*RNAi* with complete small oocytes. (K) Egg chamber size (mean ± 95% confidence intervals) in control: stage 4, 1410 ±126 μm^2 (N=23); stages 5~6, 3582 ± 375 μm^2 (N=37); stages 7~8, 10946 ± 1570 μm^2 (N=25); stage 9, 23836 ± 2518 μm^2 (N=23); egg chamber size in *shot*^{EGC}*-RNAi*: stage 4, 1620 ± 163 μm^2 (N=32); stages 5~6, 3489 ± 393 μm^2 (N=32); stages 7~8, 7700 ± 943 μm^2 (N=27); stage 9, 15305 ± 1705 μm^2 (N=22). Unpaired t-test were performed in the following groups: stage 4 control and *shot*^{EGC}-*RNAi*: p=0.0559 (n.s.); stages 5~6 control and *shot*^{EGC}*-RNAi*: p= 0.7295 (n.s.); stages 7~8 control and *shot*^{EGC}*-RNAi*: p= 0.0005 (***); stage 9 control and *shot*^{EGC}-RNAi: p<0.0001 (****).

(L) Nurse cell size (mean ± 95% confidence intervals) in control: stage 4, 919 ± 102 μm^2 (N=23); stages 5~6, 2571 ± 297 μm^2 (N=37); stages 7~8, 8100 ± 1176 μm^2 (N=25);

stage 9, 15731 ± 1421 μm^2 (N=23); nurse cell size in *shot^{EGC}-RNAi*: stage 4, 1067 ± 122.7 μm^2 (N=32); stages 5~6, 2577 ± 312 μm^2 (N=32); stages 7~8, 6040 ± 807 μm^2 (N=27); stage 9, 12394 ± 1501 μm^2 (N=22). Unpaired t-test were performed in the following groups: stage 4 control and *shot^{EGC}-RNAi*: p=0.0775 (n.s.); stages 5~6 control and *shot^{EGC}-RNAi*: p= 0.9761 (n.s.); stages 7~8 control and *shot^{EGC}-RNAi*: p= 0.0040 (**); stage 9 control and *shot^{EGC}-RNAi*: p= 0.0017 (**).

(M) Oocyte size (mean ± 95% confidence intervals) in control: stage 4, 76.3 ± 8.9 μm^2 (N=23); stages 5~6, 205.1 ± 22.9 μm^2 (N=37); stages 7~8, 808.9 ± 272.2 μm^2 (N=25); stage 9, 4749.0 ± 1015.0 μm^2 (N=23); oocyte size in *shot^{EGC}-RNAi*: stage 4, 54.2 ± 4.4 μm^2 (N=32); stages 5~6, 66.0 ± 5.7 μm^2 (N=32); stages 7~8, 76.6 ± 8.8 μm^2 (N=27); stage 9, 94.2 ± 12.4 μm^2 (N=22). Unpaired t-test were performed in the following groups: stage 4 control and *shot^{EGC}-RNAi*: p<0.0001 (****); stages 5~6 control and *shot^{EGC}-RNAi*: p<0.0001 (****); stages 7~8 control and *shot^{EGC}-RNAi*: p<0.0001 (****); stage 9 control and *shot^{EGC}-RNAi*: p<0.0001 (****). Inset, the plot of oocyte size in control stage 4 and *shot^{EGC}-RNAi* stage 4~9 egg chambers. Unpaired t-test were performed in the following groups: *shot^{EGC}-RNAi* stage 4 and stages 5~6, p=0.0014 (**); *shot^{EGC}-RNAi* stages 5~6 and stages 7~8, p= 0.0351 (*); *shot^{EGC}-RNAi* stages 7~8 and stage 9, p= 0.0180 (*).

(N) Oocyte/egg chamber ratio (mean ± 95% confidence intervals) in control: stage 4, 0.0543 ± 0.0040 (N=23); stages 5~6, 0.0583 ± 0.0050 (N=37); stages 7~8, 0.0675 ± 0.0147 (N=25); stage 9, 0.1890 ± 0.0240 (N=23); oocyte/egg chamber ratio in *shot^{EGC}-RNAi*: stage 4, 0.0357 ± 0.0038 (N=32); stages 5~6, 0.0202 ± 0.0022 (N=32); stages 7~8, 0.0109 ± 0.0017 μm^2 (N=27); stage 9, 0.0067 ± 0.0013 (N=22). Unpaired t-test were performed in the following groups: stage 4 control and *shot^{EGC}-RNAi*: p<0.0001

(****); stages 5~6 control and *shot*^{EGC}*-RNAi*: p<0.0001 (****); stages 7~8 control and *shot*^{EGC}*-RNAi*: p<0.0001 (****); stage 9 control and *shot*^{EGC}*-RNAi*: p<0.0001 (****).

(O) Oocyte nucleus size (mean ± 95% confidence intervals) in control: stage 4, 24.6 ± 3.3 μm^2 (N=23); stages 5~6, 49.0 ± 4.2 μm^2 (N=37); stages 7~8, 95.9 ± 15.5 μm^2 (N=25); stage 9, 298.7 ± 45.8 μm^2 (N=23); oocyte nucleus size in *shot*^{EGC}*-RNAi*: stage 4, 24.2 ± 1.8 μm^2 (N=32); stages 5~6, 36.1 ± 2.9 μm^2 (N=32); stages 7~8, 44.6 ± 5.6 μm^2 (N=25); stage 9, 63.6 ± 6.7 μm^2 (N=11). Unpaired t-test were performed in the following groups: stage 4 control and *shot*^{EGC}*-RNAi*: p =0.8179 (n.s.); stages 5~6 control and *shot*^{EGC}*-RNAi*: p<0.0001 (****); stages 7~8 control and *shot*^{EGC}*-RNAi*: p<0.0001 (****); stage 9 control and *shot*^{EGC}*-RNAi*: p<0.0001 (****). Inset, the plot of oocyte nucleus size in *shot*^{EGC}*-RNAi* stage 4~9 egg chambers. Unpaired t-test were performed in the following groups: *shot*^{EGC}*-RNAi* stage 4 and stages 5~6, p<0.0001 (****); *shot*^{EGC}*-RNAi* stages 5~6 and stages 7~8, p= 0.0046 (**); *shot*^{EGC}*-RNAi* stages 7~8 and stage 9, p= 0.0002 (***).

(P) Ooplasm size (mean ± 95% confidence intervals) in control: stage 4, 51.7 ± 6.8 μm^2 (N=23); stages 5~6, 156.2 ± 19.6 μm^2 (N=37); stages 7~8, 713.0 ± 259.7 μm^2 (N=25); stage 9, 4450.0 ± 975.0 μm^2 (N=23); ooplasm size in *shot*^{EGC}*-RNAi*: stage 4, 30.0 ± 3.9 μm^2 (N=32); stages 5~6, 29.9 ± 4.0 μm^2 (N=32); stages 7~8, 35.8 ± 6.0 μm^2 (N=25); stage 9, 39.4 ± 12.3 μm^2 (N=11). Unpaired t-test were performed in the following groups: stage 4 control and *shot*^{EGC}*-RNAi*: p<0.0001 (****); stages 5~6 control and *shot*^{EGC}*-RNAi*: p<0.0001 (****); stages 7~8 control and *shot*^{EGC}*-RNAi*: p<0.0001 (****); stage 9 control and *shot*^{EGC}*-RNAi*: p<0.0001 (****). Inset, the plot of ooplasm size in control stage 4 and *shot*^{EGC}*-RNAi* stage 4~9 egg chambers. Unpaired t-test were

performed in the following groups: *shot*^{EGC}*-RNAi* stage 4 and stages 5~6, p= 0.9633 (n.s.); *shot*^{EGC}*-RNAi* stages 5~6 and stages 7~8, p= 0.0863 (n.s.); *shot*^{EGC}*-RNAi* stages 7~8 and stage 9, p= 0.5298 (n.s.).

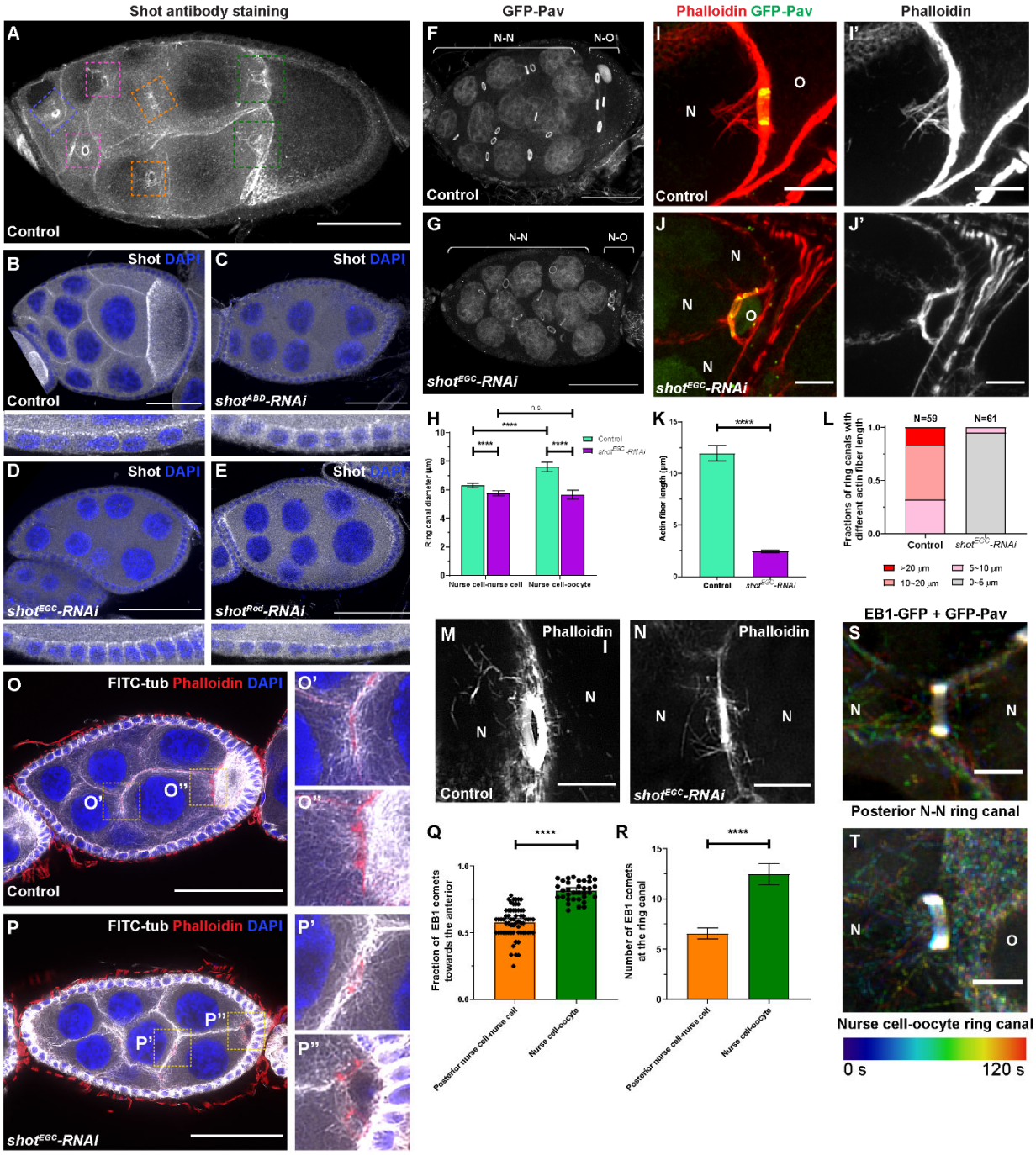

Figure S2. Characterizations of s*hot-RNAi* phenotypes and microtubule organization. Related to Figures 4 and 5.

(A-E) Shot antibody staining in control (A-B) and in three *shot-RNAi* lines (C-E). (A) Ring canals at different positions are highlighted with colored dashed boxes. (B-E) Shot

staining at the nurse cell cortex (top) or in follicle cells (bottom) are shown. To note: Shot is still localized at the apical side of the somatic follicle cells, because the *shot-RNAi* is only expressed in the germline cell. Scale bars, 50 µm.

(F-G) Representative images of ring canals in control (F) and in *shot^{EGC}-RNAi* (G). GFP-Pav strongly labels ring canals and weakly labels cell nucleus. N-N, nurse cell-nurse cell ring canals; N-O, nurse cell-oocyte ring canals. Scale bars, 50 µm.

(H) Quantification of ring canal diameters (mean ± 95% confidence intervals) in stage 8 egg chambers. Control: nurse cell-nurse cell ring canals, N=146; nurse cell-oocyte ring canals, N=60. *shot^{EGC}-RNAi*: nurse cell-nurse cell ring canals, N=147; nurse cell-oocyte ring canals, N=64. Unpaired t test with Welch's correction between the following groups: nurse cell-nurse cell ring canals (control) and nurse cell-oocyte ring canals (control), p<0.0001 (****); nurse cell-nurse cell ring canals (*shot^{EGC}-RNAi*) and nurse cell-oocyte ring canals (*shot^{EGC}-RNAi*), p=0.5031 (n.s.); nurse cell-nurse cell ring canals (control) and nurse cell-nurse cell ring canals (*shot^{EGC}-RNAi*), p<0.0001 (****); nurse cell-oocyte ring canals (control) and nurse cell-oocyte ring canals (*shot^{EGC}-RNAi*), p<0.0001 (****).

(I-J') Representative images of actin staining at the nurse cell-oocyte ring canals in stage 8 control (I-I') and *shot^{EGC}-RNAi* (J-J') egg chambers. Scale bars, 10 µm.

(K-L) Quantification of actin fibers length (K) and distribution (L) of the nurse cell-oocyte ring canals in control and in *shot^{EGC}-RNAi*. (K) For each ring canals, the lengths of the four longest actin fibers on the nurse cell side were measured. Control, 236 actin fibers from 59 ring canals; *shot^{EGC}-RNAi,* 244 actin fibers from 61 ring canals. Unpaired t test with Welch's correction between control and *shot^{EGC}-RNAi*, p<0.0001 (****). (L) The ring

canals are categorized based on the length of the longest actin fiber on the nurse cell side. Control, N=59; *shot*^{EGC}*-RNAi*, N=61.

(M-N) Representative images of actin fibers of the posterior nurse cell-nurse cell ring canals in control (M) and in *shot*^{EGC}*-RNAi* (N). Scale bars, 10 μm.

(O-P) Representative images of microtubule staining in control (O) and in *shot*^{EGC}*-RNAi* (P). microtubules are visible at the ring canals between two nurse cells (O' and P') and between the nurse cells and the oocyte (O'' and P''). Scale bars, 50 μm.

(Q) Quantification of the fractions of EB1 comets moving towards the anterior side in control. Posterior nurse cell-nurse cell ring canals, N=64; nurse cell-oocyte ring canals, N=34; unpaired t test with Welch's correction, p-value < 0.0001(****).

(R) Quantification of numbers of EB1 comets in different ring canals in control. Posterior nurse cell-nurse cell ring canals, N=64; nurse cell-oocyte ring canals, N=34; unpaired t test with Welch's correction, p-value < 0.0001 (****).

(S-T) Color-coded hyperstacks of the EB1-GFP comet movement across a posterior nurse cell-nurse cell (N-N) ring canal (S) and a nurse cell-oocyte ring canal (T). Ring canals are labeled by GFP-Pav. Scale bars, 5 μm.

N, nurse cell; O, oocyte.

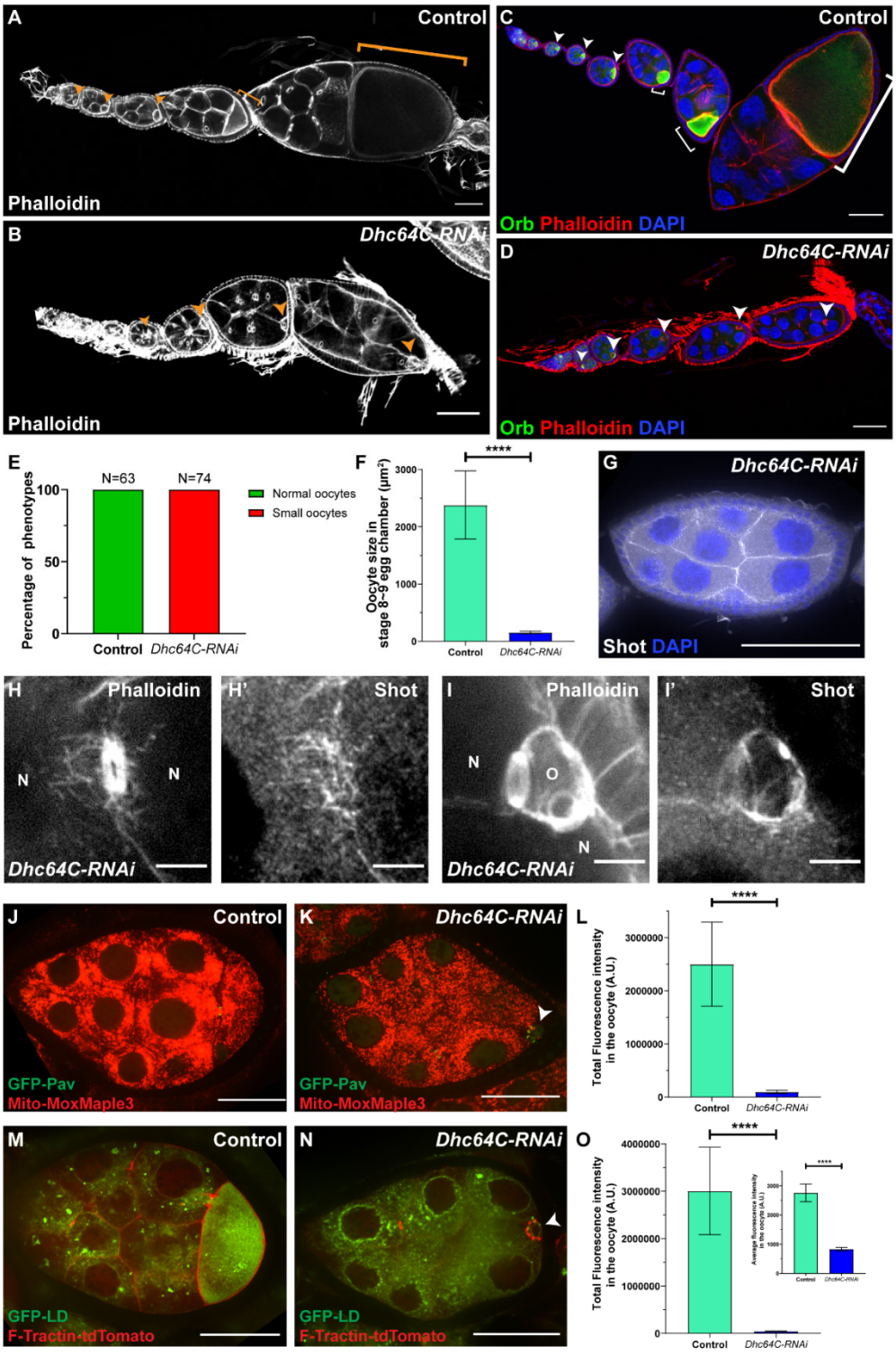

Figure S3. Cytoplasmic dynein is the main motor for cargo transport to the oocyte.

Related to Figure 6.

(A-B) Representative images of Rhodamine-conjugated phalloidin staining in control (*mat αtub-Gal4*$^{[V37]}$/+) and *dynein-RNAi* (*UAS-Dhc64C-RNAi*/+; *mat αtub-Gal4*$^{[V37]}$/+). Normal oocyte growth in control, shown by orange arrowheads and brackets (A); oocytes remain small in *Dhc64C-RNAi*, shown by orange arrowheads (B). Scale bars, 50 μm.

(C-D) Representative images of Orb staining in control and (*mat αtub-Gal4*$^{[V37]}$/+) and *dynein-RNAi* (*UAS-Dhc64C-RNAi*/+; *mat αtub-Gal4*$^{[V37]}$/+). Orb concentration is observed in control oocytes starting stage 1 to stage 10, shown by white arrowheads and brackets (C). To note: Orb staining is visibly dimmer in the stage 10B oocyte as the fast increase of oocyte volume dilutes the Orb concentration. Orb concentration is gradually lost in the *dynein-RNAi* oocytes, shown by white arrowheads (D). Scale bars, 50 μm.

(E) Summary of oocyte phenotypes in control (N=63) and *Dhc64C-RNAi* (N=74).

(F) Quantifications of the oocyte size in control (N=34) and *Dhc64C-RNAi* (N=56) stage 8~early stage 9 egg chambers. Unpaired t test with Welch's correction between control and *Dhc64C-RNAi*: $p<0.0001$ (****).

(G-I') Representative images of Shot staining in *Dhc64C-RNAi*. A whole egg chamber (G) and zoom-in areas of a posterior nurse cell-nurse cell ring canal (H-H') and nurse cell-oocyte ring canals (I-I'). Scale bars, 50 μm (G) or 5 μm (H-I'). N, nurse cell; O, oocyte.

(J-L) Mitochondria localization in control (J) and in *Dhc64C-RNAi* (K). Mitochondria are labeled with Mito-MoxMaple3 (red channel, after global photoconversion) and ring

canals are labeled with GFP-Pav. The small oocyte in *Dhc64C-RNAi* is pointed with a white arrowhead (K). (L) Quantification of total mitochondria fluorescence intensity (mean ± 95% confidence interval) in control (N=34) and in *Dhc64C-RNAi* (N=56) oocytes of stage 8 egg chambers. Unpaired t test with Welch's correction, p-value < 0.0001 (****). Scale bars, 50 μm. See also Video 11.

(M-O) The localization of lipid droplets in control (M) and in *Dhc64C-RNAi* (N). Lipid droplets are labeled with GFP-LD and ring canals are labeled with F-Tractin-tdTomato. The small oocyte in *Dhc64C-RNAi* is pointed with a white arrowhead (N). (O) Quantifications of total fluorescence intensity and average fluorescence intensity (inset) of lipid droplets (mean ± 95% confidence interval) in control (N=21) and in *Dhc64C-RNAi* (N=46) oocytes of stage 8 egg chambers. Unpaired t test with Welch's correction of total fluorescence intensity of GFP-LD, p-value < 0.0001 (****); Unpaired t test with Welch's correction of average fluorescence intensity of GFP-LD, p-value < 0.0001 (****). Scale bars, 50 μm.